The British Journal of Radiology, 83 (2010), 1080–1086

PICTORIAL REVIEW

MRI findings of uncommon non-hepatocyte origin primary liver tumours with pathological correlation

[1,3]Y C KIM, MD, [1]M-S PARK, MD, [1]Y E CHUNG, MD, [1]M-J KIM, MD, [2]Y N PARK, MD, [1]J-H KANG, MD, [1]K A KIM, MD and [1]K W KIM, MD

[1]*Department of Diagnostic Radiology, Institute of Gastroenterology, Research Institute of Radiological Science, Yonsei University Health System, Seoul, Republic of Korea,* [2]*Department of Pathology, Yonsei University Health System, Seoul, Republic of Korea and* [3]*Department of Radiology, Ajou University School of Medicine, Suwan, Republic of Korea*

ABSTRACT. The objective of this article was to illustrate the MRI findings of uncommon non-hepatocyte origin primary liver tumours, correlate them with the pathological features and discuss differential diagnoses. In conclusion, the MRI findings of uncommon benign and malignant non-hepatocyte-origin primary liver tumours vary. Awareness of characteristic MRI features can aid differential diagnosis and prevent unnecessary surgery.

Received 28 October 2009
Revised 26 January 2010
Accepted 22 March 2010

DOI: 10.1259/bjr/61140265

MRI has become an indispensable modality for the evaluation of focal liver lesions. The absence of ionizing radiation, unparalleled soft-tissue contrast and the common use of liver-specific contrast agents are major advantages over other imaging techniques. Two gadolinium chelates — Gd-EOB-DTPA (gadolinium ethoxybenzyl diethylenetriaminepentaacectic acid; Primovist®) and Gd-BOPTA (gadobenate dimeglumine; Multihance®) — have the properties of both an extracellular agent and a hepatobiliary agent, with the excretion into the biliary system of 50% and 3–5%, respectively [1, 2].

In our institution, contrast-enhanced MRI was performed using a breath-hold three-dimensional gradient-echo sequence with fat saturation after an intravenous bolus of 0.025 mmol kg^{-1} Gd-EOB-DTPA and 0.1 mmol kg^{-1} Gd-BOPTA followed by a saline flush of 20 ml. The three-phase dynamic images were obtained at 30–35 s for arterial phase and 65–70 s for portal venous phase and 5 min for equilibrium phase after the injection of Gd-EOB-DTPA or Gd-BOPTA. Hepatobiliary phase images were obtained 20 min after Gd-EOB-DTPA and 107–195 min (mean 138 min) after Gd-BOPTA injection.

Primary liver tumours may be classified into hepatocellular tumours, biliary tumours, mesenchymal tumours and other tumours, according to the origin of cells. Some hepatic tumours, especially uncommon tumours, can be difficult to characterise, and MRI has been frequently used to refine differential diagnoses to avoid unnecessary surgery and correct inappropriate follow-up. In this article, we will illustrate MRI findings of uncommon benign and malignant non-hepatocyte origin primary liver tumours, correlate them with pathological findings and discuss their impact on differential diagnosis.

Address correspondence to: M-S Park, Department of Diagnostic Radiology, Yonsei University Health System, Seodaemun-gu, Seongsanno 250 (Shinchon-dong 134), Seoul 120-752, Republic of Korea. E-mail: radpms@yuhs.ac

Biliary hepatic tumours

Primary hepatic neuroendocrine tumour

Just 55 cases of primary hepatic neuroendocrine tumour (NET) have been described in current literature [3]. Although the pathogenesis of primary hepatic NET has not been established, one significant hypothesis suggests that tumour cells might originate from the neuroendocrine cells in the epithelium of the intrahepatic bile duct [4, 5]. These tumours are usually non-functioning neoplasms. Primary hepatic NET usually occurs as well-demarcated solitary masses with internal fibrous septa and capsule.

CT demonstrates a well-defined, low attenuated mass with heterogeneous enhancement. MRI shows variable high signal intensity on T_2 weighted images depending on the amount of fibrosis, calcification, haemorrhage and necrosis, and relatively low signal intensity on T_1 weighted images compared with the liver parenchyma. On dynamic contrast-enhanced study, early enhancement on arterial phase and washout on portal venous phase are usually seen. On equilibrium phase (5 min after the injection of the contrast), contrast accumulation in the centre may be seen in those with a central scar (Figure 1) [6–8].

Bile duct adenoma (peribiliary gland hamartoma)

Bile duct adenoma (BDA) is a rare benign lesion of the liver. Previously, BDA was considered a true neoplasm, but recent reports suggest that BDA originates from

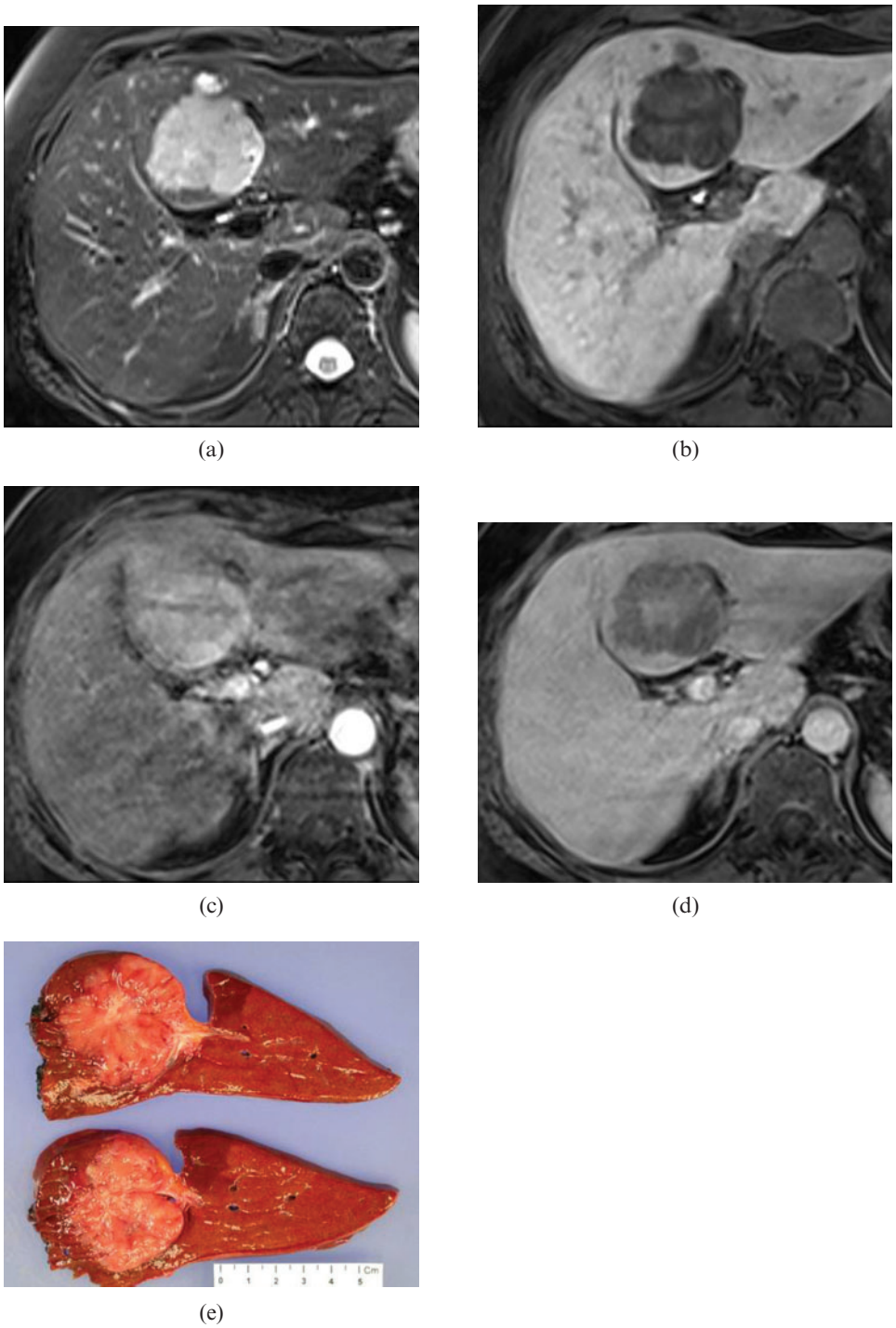

Figure 1. A 54-year-old woman with primary hepatic neuroendocrine tumour. (a) T_2 weighted MRI shows a primary lobulated and hyperintense lesion with a small adjacent satellite nodule in the segment 4 of the liver. (b) On T_1 weighted image, the mass lesion shows hypointensity. (c) On arterial phase of gadolinium ethoxybenzyl diethylenetriaminepentaacectic acid (Gd-EOB-DTPA) enhanced T_1 weighted image, the mass lesions show the moderate enhancement. (d) On equilibrium phase, the mass lesion shows defect with central enhancement. (e) Surgical specimen shows a protruded mass with fibrous capsule and central scar at the posterior wall of the medial inferior area.

peribiliary gland precursor tissue that has failed to organise into a mature gland (a so-called peribiliary gland hamartoma). BDA usually presents as a single nodule measuring less than 2 cm in diameter located in the subcapsular area of the liver [9]. Histologically, BDA is a well-circumscribed, non-encapsulated nodule composed of aggregates of bile ductules in the connective tissue stroma with various degrees of chronic inflammation and collagenisation.

In contrast to biliary hamartoma, BDA is usually single, does not show cystic changes and contains bile within the ductules. Microscopically, fibrosis is denser in the centre while bile ductules with abundant extracellular spaces are denser in the periphery. There are very few reports on the

radiological findings of BDA in the literature. In our case, the BDA was hyperintense or isointense in the periphery, and hypointense in the central area on emph>emph type="inf">2 weighted MRI. In dynamic images, BDA shows delayed and prolonged enhancement, especially in the central portion on the equilibrium phase (Figure 2) [10, 11].

Biliary hamartoma (Von Meyenberg complex)

Biliary hamartoma (BH), a ductal plate malformation, consists of numerous small (usually <0.5 cm), irregular-shaped, dilated ductules embedded in a dense fibrous stroma. The ductules are lined by cuboidal or flattened epithelial cells and are not connected to the biliary system [12]. On ultrasound, BH appear as numerous tiny hyperechoic or hypoechoic foci that are scattered throughout the liver. On CT, BH appear as small, low-attenuating lesions with no enhancement. On MRI, BH are usually seen as innumerable hyperintense nodules that do not communicate with the biliary system (Figure 3). In one of our cases, however, an unusual form of BH presented as a single nodule. The nodule appeared hyperintense on T_2 weighted images and hypointense on T_1 weighted images (Figure 4).

Non-epithelial tumours

Lymphangioepitheloima-like carcinoma

Lymphangioepitheloima-like carcinoma (LELC) is a rare, undifferentiated carcinoma with intense lymphoplasmacytoid stroma, originally described in the nasopharynx [13]. Primary LELC has been identified as the variant type of cholangiocarcinoma. Although LELC shows equivocal association with Epstein–Barr virus (EBV) in diverse organs, EBV may play an important role in the pathogenesis [14].

On ultrasound, LELC shows low echogenicity. CT scan demonstrates low density without enhancement. To date, the MRI appearances have not been reported. In our case, the lobulated mass lesion appeared slightly hyperintense on T_2 weighted images and hypointense on T_1 weighted images. Contrast enhanced T_1 weighted

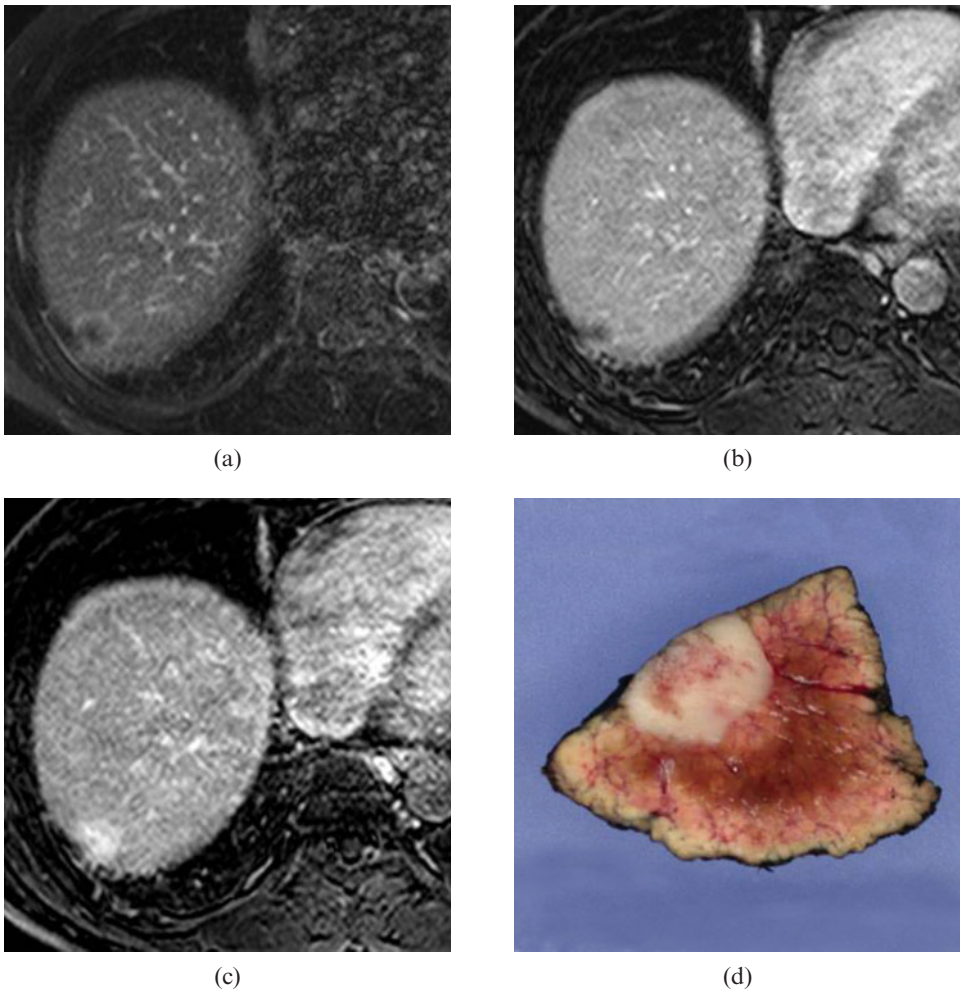

Figure 2. A 53-year-old man with a bile duct adenoma. (a) The axial T_2 weighted image shows a three-layered, hyper-iso-hypointense pattern from the periphery to the centre, round lesion at the subcapsular area of the liver. (b) On portal venous phase of Gd-BOPTA-enhanced T_1 weighted image, the mass shows thin hyperintense incomplete rim-like outer layer, thick isointense middle layer and hypointense central area. (c) On equilibrium phase, the mass shows delayed and prolonged enhancement, especially in the centre. (d) The surgical specimen shows a round, pinkish solid mass composed of aggregated bile ductules with central denser fibrosis area.

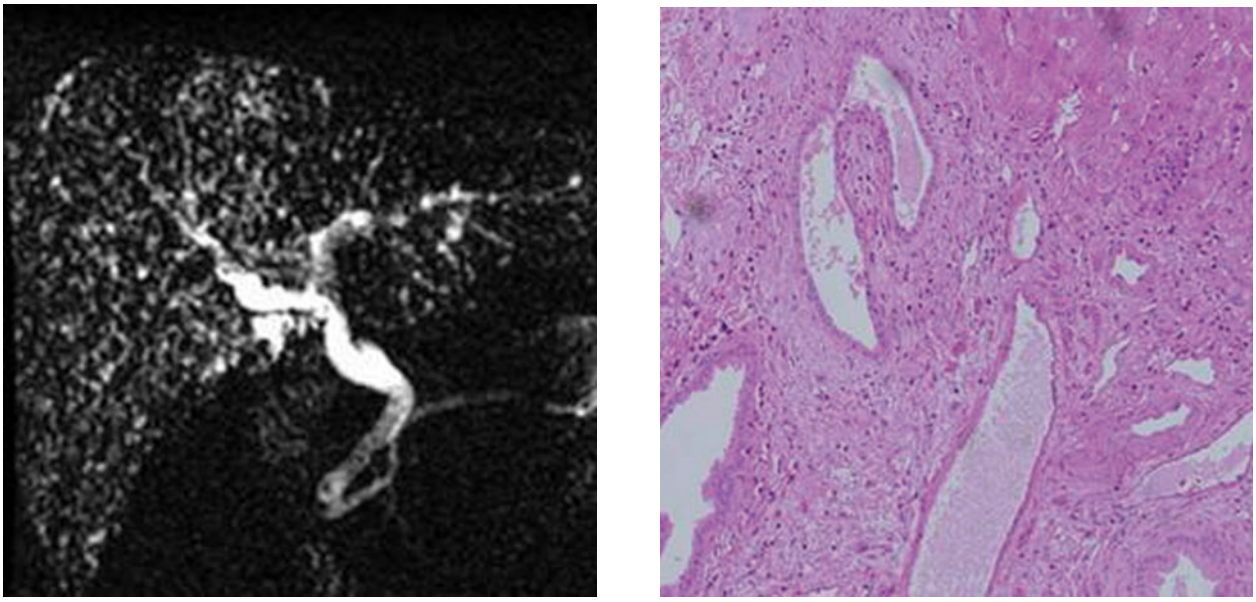

(a) (b)

Figure 3. A 74-year-old man with biliary hamartomas. (a) On magnetic resonance cholangiopancreatography, numerous small hyperintense foci are found in the liver. (b) Microscopic specimen (original magnification $\times$100; haemotoxylin and eosin stain) shows an irregular gland with a low columnar epithelium in a fibrous stroma that is compatible with biliary hamartomas.

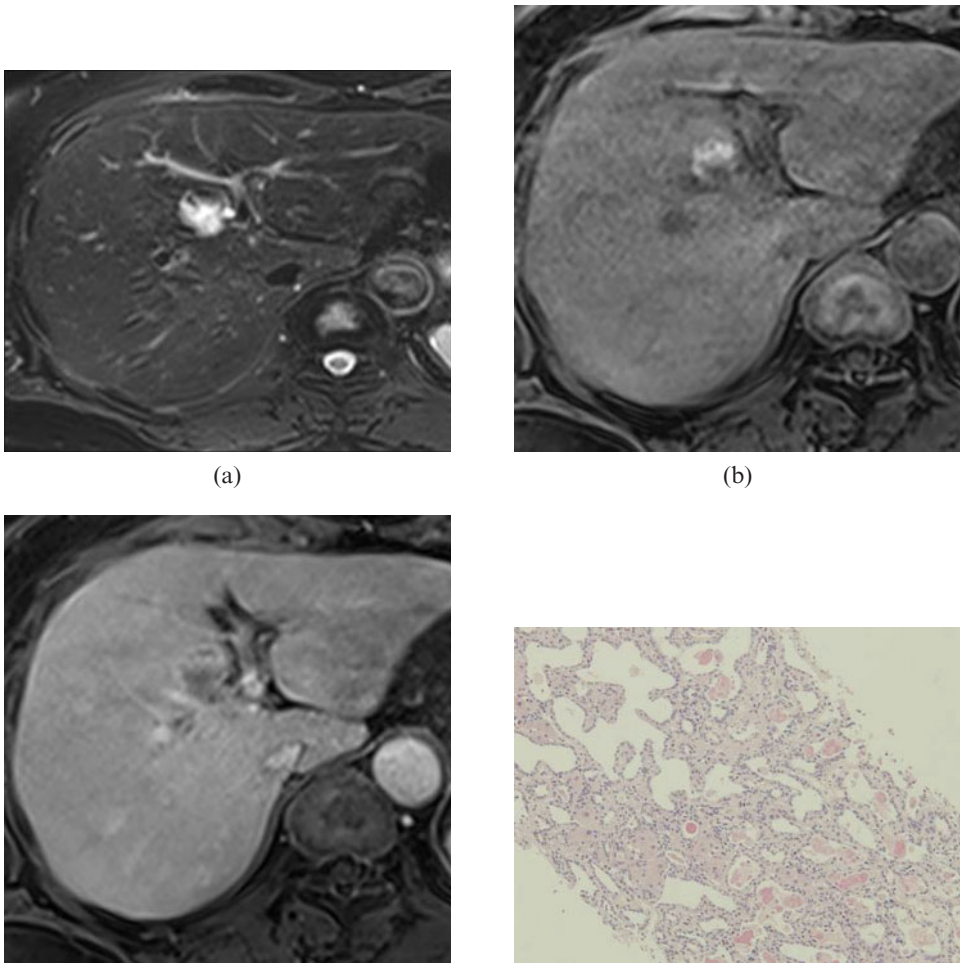

(a) (b)

(c) (d)

Figure 4. A 53-year-old man with a solitary biliary hamartoma. (a) The T_2 weighted image shows a hyperintense nodule. (b) On T_1 weighted image, the mass shows heterogeneous hyperintensity. (c) On equilibrium phase of Gd-EOB-DTPA enhanced T_1 weighted image, the mass shows thin peripheral rim enhancement. (d) The microscopic specimen (original magnification $\times$100; haemotoxylin and eosin stain) shows irregular-shaped glands with short columnar epithelium in fibrous stroma, compatible with a biliary hamartoma.

MRI showed progressive enhancement in the periphery of the lesion. On hepatobilliary phase, the lesion shows hypointensity with a lobulated margin. However, the imaging features on MRI of this entity will need to be confirmed by future reports (Figure 5).

Schwannoma

Hepatic schwannoma is a very rare benign mesenchymal tumour that originates from a variety of hepatic sympathetic and parasympathetic nerves distributed among the intralobular connective tissues, portal vein and hepatic arteries. This tumour is usually found along the branches of the portal tracts [15, 16]. The histological hallmarks of a schwannoma are a true capsule and a mixture of Antoni A (hypercellular area) and Antoni B (hypocellular area with a more myxoid matrix and water content) regions. This tumour sometimes undergoes secondary degeneration, resulting in cystic changes, calcification deposits and haemorrhage formation [17].

On MRI, a schwannoma usually presents as an encapsulated, well-demarcated round or ovoid mass. The signal intensity on T_1 and T_2 weighted images varies depending on the proportion of Antoni A and Antoni B regions with the presence of secondary degeneration. Schwannoma usually shows non-homogeneous high signal intensity on T_2 weighted images, low to intermediate signal intensity on T_1 weighted images and variable enhancement on post-contrast images owing to the mixture of Antoni A and B (Figure 6) [18].

Inflammatory pseudotumor

A hepatic inflammatory pseudotumour (IPT) is an unusual lesion composed of proliferating fibrovascular tissue infiltrated by inflammatory cells, and has the

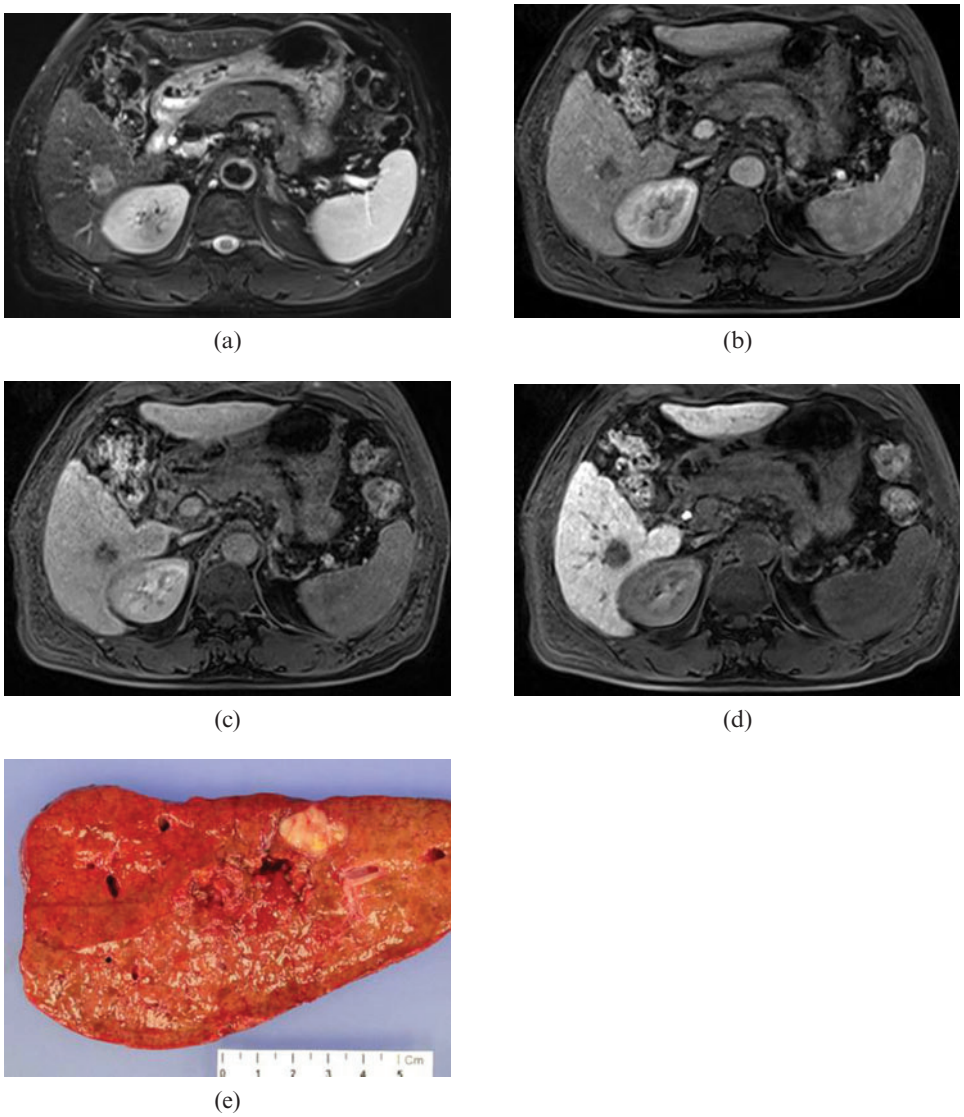

Figure 5. A 61-year-old man with lymphangioepithelioma-like carcinoma. (a) T_2 weighted image shows a slightly hyperintense nodular lesion in the segment 6 of the liver. (b) On arterial phase of Gd-EOB-DTPA enhanced T_1 weighted image, minimal enhancement is noted in the posterior aspect of lesion. (c) On equilibrium phase, the mass shows progressive enhancement in the periphery of the lesion. (d) On hepatobilliary phase, the mass shows hypointense with a lobulated margin. (e) Surgical specimen reveals a light yellow-coloured multinodular confluent type of mass, measuring 2.2×1.8 cm.

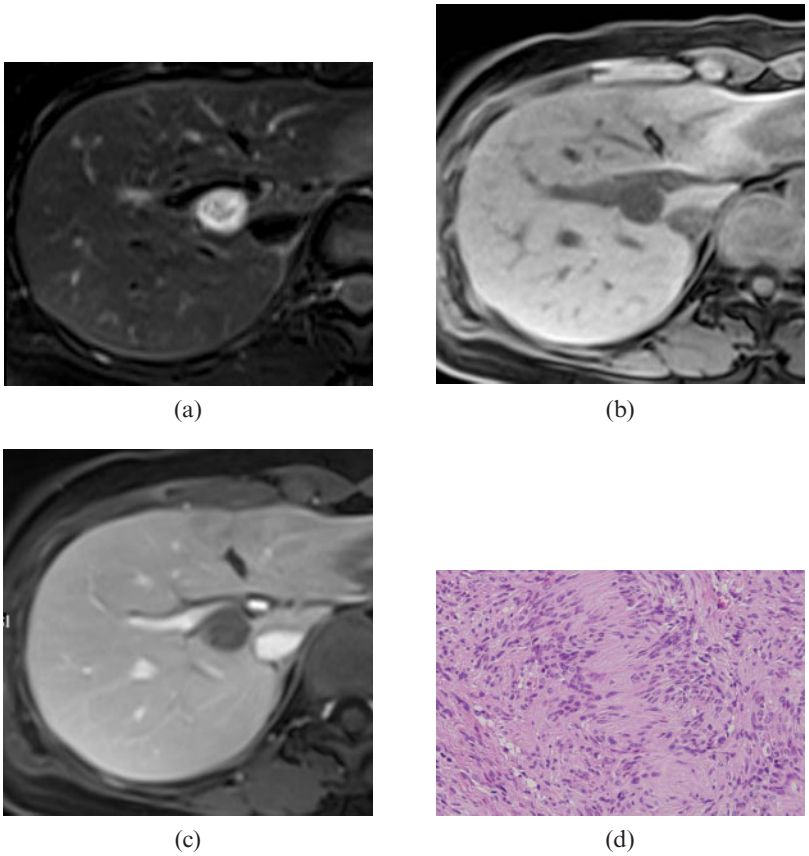

Figure 6. A 29-year-old woman with a schwannoma. (a) The T_2 weighted MRI shows a well-demarcated round heterogeneous, hyperintense nodule. (b) The T_1 weighted MRI shows a hypointense nodule. (c) No enhancement of the mass is seen on portal venous phase of Gd-EOB-DTPA enhanced T_1 weighted MRI. (d) The microscopic specimen (original magnification $\times 200$; haemotoxylin and eosin) of surgical specimen has storiform bundles of spindle cells arranged in whorls and surrounded by a fibrous capsule.

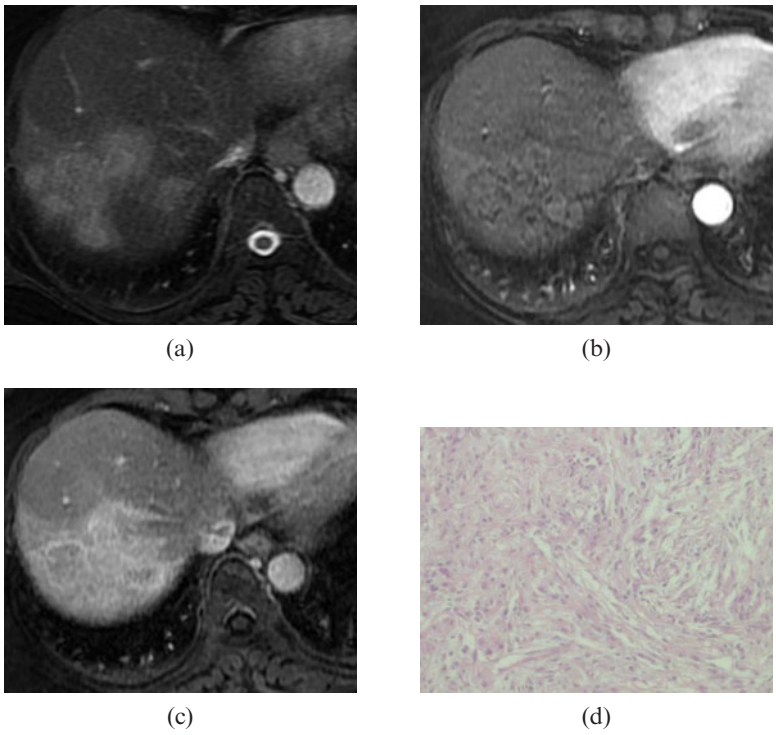

Figure 7. A 66-year-old woman with an inflammatory pseudotumour. (a) The T_2 weighted image shows an ill-defined hyperintense lobulated mass in the liver. (b and c) On arterial and equilibrium phases of Gd-BOPTA enhanced T_1 weighted image, the mass shows inhomogeneous gradual delayed enhancement (d) The microscopic specimen ($\times 200$; haemotoxylin and eosin stain) of surgical specimen shows lymphocyte infiltration and fibroblastic proliferation of the surrounding connective tissue.

potential for recurrence, persistent local growth and spontaneous regression [19]. IPT can develop secondary to recurrent cholangitis or portal vein infection, but the pathogenesis is still unclear [19]. On MRI, these lesions can appear as solitary or multiple nodular lesions with hypointensity or isointensity on T_1 weighted images, isointensity or slight hyperintensity on T_2 weighted images and variable enhancement on dynamic images owing to the wide range of vascularity – from avascular to hypervascular (Figure 7) [20]. Inaba et al [19] suggested that the absence of enhancement on arterial phase may be the key differential point of IPT from other hypervascular tumours, such as hepatocellular carcinoma. However, it is very difficult to differentiate these tumours from other malignant tumours, especially cholangiocarcinoma, which usually shows progressive enhancement [20].

Conclusions

MRI findings of uncommon non-hepatocyte benign and malignant tumours in the liver vary, and can be either specific or nonspecific. However, awareness of the pathological and MRI findings of these tumours is important not only for differential diagnosis from malignant focal lesions, but also to avoid unnecessary treatment.

Acknowledgments

This study was supported by a grant of the Korea Healthcare Technology Research and Development Project, Ministry for Health, WelFare and Family Affairs, Republic of Korea (AO84120).

References

1. Planchamp C, Hadengue A, Stieger B, Bourquin J, Vonlaufen A, Frossard JL, et al. Function of both sinusoidal and canalicular transporters controls the concentration of organic anions within hepatocytes. Mol Pharmacol 2007;71:1089–97.
2. Grazioli L, Morana G, Kirchin MA, Schneider G. Accurate differentiation of focal nodular hyperplasia from hepatic adenoma at gadobenate dimeglumine-enhanced MR imaging: prospective study. Radiology 2005;236:166–77.
3. Dala R, Shoosmith J, Lilenbaum R, Cabello-Inchausti B. Primary hepatic neuroendocrine carcinoma: an underdiagnosed entity. Ann Diagn Pathol 2006;10:28–31.
4. Ishida M, Seki K, Tatsuzawa A, Katayama K, Hirose K, Azuma T, et al. Primary hepatic neuroendocrine carcinoma coexisting with hepatocellular carcinoma in hepatitis C liver cirrhosis: report of a case. Surg Today 2003;33:214–18.
5. Hwang S, Lee YJ, Lee SG, Kim CW, Kim KH, Ahn CS, et al. Surgical treatment of primary neuroendocrine tumors of the liver. J Gastrointest Surg 2008;12:725–30.
6. van der Hoef M, Crook DW, Marincek B, Weishaupt D. Primary neuroendocrine tumors of the liver: MRI features in two cases. Abdom Imaging 2004;29:77–81.
7. Dromain C, de Baere T, Baudin E, Galline J, Ducreux M, Boige V, et al. MR imaging of hepatic metastases caused by neuroendocrine tumors: comparing four techniques. AJR Am J Roentgenol 2003;180:121–8.
8. Hussain S, Gollan J, Richard C. Liver MRI: Correlation with Other Imaging Modalities and Histopathology: Springer Verlag; 2007.
9. Allaire GS, Rabin L, Ishak KG, Sesterhenn IA. Bile duct adenoma. A study of 152 cases. Am J Surg Pathol 1988;12:708–15.
10. Tajima T, Honda H, Kuroiwa T, Yoshimitsu K, Irie H, Aibe H, et al. Radiologic features of intrahepatic bile duct adenoma: a look at the surface of the liver. J Comput Assist Tomogr 1999;23:690–5.
11. Maeda E, Uozumi K, Kato N, Akahane M, Inoh S, Inoue Y, et al. Magnetic resonance findings of bile duct adenoma with calcification. Radiat Med 2006;24:459–62.
12. Kakar SB, Burgart LJ. Tumours of the biliary system. Curr Diagn Pathol 2005;11:34–43.
13. Jeng YM, Chen CL, Hsu HC. Lymphoepithelioma-like cholangiocarcinoma: an Epstein-Barr virus-associated tumor. Am J Surg Pathol 2001;25:516–20.
14. Min HS, Shin E, Jang JJ. [Carcinoma with predominant lymphoid stroma in hepatobiliary system—report of 2 cases]. Korean J Hepatol 2007;13:222–7.
15. Lee WH, Kim TH, You SS, Choi SP, Min HJ, Kim HJ, et al. Benign schwannoma of the liver: a case report. J Korean Med Sci 2008;23:727–30.
16. Park MK, Lee KT, Choi YS, Shin DH, Lee JY, Lee JK, et al. [A case of benign schwannoma in the porta hepatis]. Korean J Gastroenterol 2006;47:164–7.
17. Theodosopoulos T, Stafyla VK, Tsiantoula P, Yiallourou A, Marinis A, Kondi-Pafitis A, et al. Special problems encountering surgical management of large retroperitoneal schwannomas. World J Surg Oncol 2008;6:107.
18. Momtahen AJ, Akduman EI, Balci NC, Fattahi R, Havlioglu N. Liver schwannoma: findings on MRI. Magn Reson Imaging 2008;26:1442–5.
19. Inaba K, Suzuki S, Yokoi Y, Ota S, Nakamura T, Konno H, et al. Hepatic inflammatory pseudotumor mimicking intrahepatic cholangiocarcinoma: report of a case. Surg Today 2003;33:714–17.
20. Fukuya T, Honda H, Matsumata T, Kawanami T, Shimoda Y, Muranaka T, et al. Diagnosis of inflammatory pseudotumor of the liver: value of CT. AJR Am J Roentgenol 1994;163:1087–91.